UNIVERSITY OF MICHIGAN BIOLOGICAL STATION

Analysis of Glyoxal Concentrations Among a Deciduous Forest Canopy

Erik D. Johnson
Saint Olaf College
August 15th, 2008

Mentors:

Aster Kammrath, University of Wisconsin-Madison

Melissa Galloway, University of Wisconsin-Madison

2008 NSF REU Program

Introduction

Knowledge of the global climate and the course that it will take is becoming increasingly important as anthropogenic emissions consistently increase each year. Human emissions direct atmospheric chemistry by changing the global budgets of ozone, carbon dioxide, VOCs, etc. and manipulating the effects of biogenic emissions. It is important for the scientific community to improve predictive capabilities for climate change, tropospheric ozone, and aerosol concentrations as these are important factors in human health, ecosystems, and the economy. Aerosol has recently come into focus as a vital source of information surrounding climate change, but more work is required to quantify the role of aerosol within large scale global climate change. In particular, the influence of aerosol is recognized as the largest uncertainty in IPCC's evaluations of climate forcing. Current models used to calculate secondary organic aerosol (SOA) concentrations commonly underestimate by an order of magnitude when compared with field measurements.

Directly related to the formation of aerosol appears to be biogenic volatile organic compounds (BVOCs), particularly isoprene (C_5H_8) and terpenes. The emission of BVOCs affects atmospheric chemistry by enhancing ozone formation in polluted areas, contributing to tropospheric aerosol deposition (Seinfeld and Pandis, 1998), and reducing the overall oxidizing capacity of the troposphere. Emissions of isoprene are the largest of any BVOC except for methane, making up almost half of all global BVOC emissions (Kanakidou et al., 2005) and estimated to be on the order of 500 Tg/year for the world (Guenther et al. 2006). Isoprene production follows a general diurnal trend, with heavy dependence on light and temperature. Maximum release occurs during the sunny daytime hours followed by characteristic nighttime decay (Hurst et al., 2001). Numerous isoprene oxidation pathways have been recognized, making it difficult to understand precisely what products result from different atmospheric and weather conditions.

Recently, a valuable tool for the detection of part-per-trillion mixing concentrations of glyoxal, the smallest α-dicarbonyl, has been developed by the Keutsch group (University of Wisconsin-Madison). Glyoxal is of interest because it is one of the most frequently occuring higher generation oxidation products of isoprene. At the same time, measurements of glyoxal illustrate the complexity of isoprene oxidation chemistry and can be thought of as

a general marker of SOA formation as deposition onto aerosol has been observed (Fu, et al. Submitted 2007). Glyoxal is also a valuable indicator of the persistently active VOC chemistry in air due to its relatively low atmospheric lifetime of around 1.3 hours (Volkamer et al. 2005). Hence, daytime changes in glyoxal concentrations are a marker for determining the dynamic nature of aerosol and isoprene fluctuations in the atmosphere. As glyoxal is a secondary product of isoprene, preliminary observations of concentrations have seen a similar diurnal trend to that of isoprene, with a peak generally occurring around mid-afternoon and decay taking place after sunset. Nighttime concentrations are typically steady and quite low.

Several factors shape the creation and destruction of glyoxal in the atmosphere. Some of the parameters that are recognized to have the greatest influence on the production of glyoxal include: OH radical concentrations (Volkamer, et al. 2001), ozone and isoprene concentrations (Spaulding et al. 2003), and incoming UV radiation. Major sinks of glyoxal are believed to include: reaction with the OH radical (Becker 2001), deposition onto aerosol (Liggio et al. 2005), and loss via photolysis (Tadic et al. 2006).

The purpose of this study is to determine whether or not differences exist in glyoxal concentrations across different elevations. Several factors could possibly contribute to variability, notably different weather conditions which correspond to variations in temperature, precipitation, humidity, intensity of UV radiation, and wind masses. One may expect to see higher daytime concentrations of glyoxal above the canopy rather than below as, in rural areas, it is primarily produced from isoprene that is emitted from the stomata of trees. On overcast days, the difference between the concentrations is anticipated to be smaller because less isoprene will be emitted above the canopy, while more diffuse radiation may cause higher photosynthetic rates among certain species of undergrowth and increase the amount of isoprene, and consequently the amount of glyoxal that is observed below the canopy (Knohl et al. 2008). More light reaching under-story may also increase photosynthesis rates among trees such as white pine, releasing MBO, which will also produce glyoxal as oxidation product (Grosjean 1990). On rainy days, almost no glyoxal is expected because high water solubility results in very efficient wet deposition (Matsunaga et al. 2007). Other cases may involve changing wind patterns that in turn alter the concentrations of species liable to react with glyoxal precursers.

Following collection of data, a model will be created to establish a foundation for predictions of glyoxal concentrations based on general weather conditions, elevation, and isoprene concentrations. The model will then be adjusted to fit the measured concentrations found in the field.

Materials and Methods

Location

The University of Michigan Biological Station is located in Northern Michigan approximately 20 miles south of Mackinaw City, MI, and east of Pellston, MI (approximately 45.56N, 84.72W). Relatively low populations of the surrounding area theoretically keep anthropogenic emissions to a minimum, with Pellston Regional Airport (6.8 miles to the west) possibly having some influence on local air quality. Douglas Lake, a moderately large body of water (3395 acres), lies less than a mile northeast of the collection site. Measurements of glyoxal will be made at the PROPHET (Program for Research on Oxidants: PHotochemistry, Emissions, and Transport) Laboratory in a wooded area west of the University of Michigan Biological Station itself. The surrounding forest consists primarily of bigtooth aspen, red oak, paper birch, American beech, and white pine, with bigtooth aspen being the major species present.

Figure 1. PROPHET tower

The PROPHET tower consists of scaffolding constructed to an elevation of 31.4 meters (Figure 1), which rises up from the west side of a ground-based laboratory. Ambient air is drawn from the top (33 meters) through a glass sampling manifold that is 5 cm in diameter down to the lab below. The collected air takes approximately 2 seconds to travel from top to bottom in the manifold, where it can be routed to different instruments (Carroll et al. 2001). Instrumentation can also be placed on the tower itself, to prevent any line-losses that may occur.

Data Collection

Due to the relatively dynamic nature of glyoxal in the atmosphere, measurements were taken using the Madison Laser-Induced Phosphorescence (LIP) instrument. Calibrations throughout the sampling period determined that the Madison LIP instrument had a one minute limit of detection of approximately 6 ppt, which allowed for the sampling of expected ambient mixing concentrations of glyoxal in a rural setting. Another characteristic of the instrument that was especially important in this study was the option of flowing ambient air through multiple inlets. This provided the opportunity to take continuous measurements throughout the day and monitor multiple diurnal profiles. The instrument was employed at the PROPHET tower to record fluctuating glyoxal concentrations from two altitudes in a deciduous forest. Measurements alternated according to a 3:1 pattern, where 30 minutes will be spent collecting from the main inlet, and 10 minutes was spent collecting from the alternate inlet. Each location was constantly sampled from the beginning of the study. Instrument calibrations always take place during the night, when glyoxal concentrations remain very low and relatively constant so that ambient concentrations do not lead to inaccuracies in the calibration factor.

Collections of above canopy air were regularly drawn from the glass manifold on PROPHET tower into the primary inlet of the LIP. For the purpose of this experiment, an additional inlet was brought up the tower, which created an extended path for the alternate inlet. Although the total length of the Teflon-coated inlet tubing was approximately equal to that of the manifold (~30 meters), it was not permanently fixed to the tower. Thus, its height was adjusted to create a coarse profile of glyoxal concentrations through the canopy, while the manifold consistently took measurements from above the canopy. Preliminary observations demonstrated that there was not a significant difference between measurements collected from the manifold and the Teflon-coated tubing when air was drawn through both from the top of the tower. Initial measurements were also alternated between a 5 meter inlet tube and the 30 meter tube, as glyoxal is typically considered a relatively “sticky” species. This test established that there were no significant losses through the longer tubing. As there was no difference between the glass manifold and the longer tubing, it can be assumed that measurements comparing the glass manifold with the shorter tubing would show no significant differences.

Instrumentation

The following is a brief description of the custom built LIP instrument that was used to collect data in this experiment. A more detailed explanation of the LIP instrument is provided by "Laser-Induced Phosphorescence for the in Situ Detection of Glyoxal at Part per Trillion Mixing Ratios" by Huisman, et al. (Published 2008).

Detection of glyoxal is based on an excitation pathway that allows the molecule to absorb energy, enter a singlet state, collide with other molecules and enter a unique triplet state, and finally release a photon to reassume its ground state. The Madison LIP instrument utilizes a Ti:sapphire laser tuned to a very specific range of wavelengths surrounding 440.25nm, which provides an energetic pathway for glyoxal molecules to enter a singlet state. Following this excitation, a partial relaxation allows glyoxal cross the threshold to a di-radical triplet state with a lifetime of approximately 10 microseconds at 100 Torr. At this point, around 1/3 of the originally excited molecules will remain in the triplet state, while the others settle to lower energetic levels.

Gathering of ambient air begins at an outdoor collection point, where atmospheric glyoxal enters inlet tubing under vacuum and travels into the LIP instrument at a rate of 31 SLM with a pressure of approximately 100 Torr, as controlled by an electronic needle valve and confirmed by an MKS Baratron. Gas then flows through the white cell where it encounters a brief laser pulse (30 ns) and glyoxal molecules are brought to an excited state. Glyoxal phosphorescence is collected through a 520nm bandpass filter to minimize possible interference from the fluorescence of non-target particles, and Rayleigh, Raman, and particle scatter. Temporally gated collection from 2.5-37 microseconds following laser excitation also increases specificity for glyoxal, due to the relatively consistent phosphorescence profile of glyoxal and also because scattering and fluorescence are fast processes that are complete within 2.5 microseconds before gated detection begins.

Data recognition is associated with two major points of absorbance, a maximum collection point at 440.26nm and nearby minimum at 440.23nm (termed "online" and "offline" respectively). "Online" corresponds to a maximum in the absorption profile, or a wavelength at which many molecules are excited to the singlet state. This, in turn means more molecules ending up in the triplet state and, therefore more phosphorescence. Alternatively, the offline position corresponds to a minimum in the absorption spectrum.

Less absorption means fewer molecules excited to the singlet state, which means less phosphorescence and lower signal from the PMT. Data is gathered every second and averaged every minute for 40 s online followed by 20 s offline, to establish a background for comparison. A scan over the entire excitation region (440.2-440.3nm) is taken every half hour to ensure that the laser's position has not drifted. The laser is also shuttered for a period of 20 s and counts are taken to check for light leaks into the cell.

Calibration of the LIP device is accomplished by flushing the cell three times with small amounts of calibrant gas of a known concentration as determined by cavity ringdown spectroscopy. LIP measurements are then taken at various flow rates of calibrant gas (4, 10 and 7 sccm diluted by 31 SLM of ambient air) after flow has stabilized. Three flow rates are used to plot a calibration curve of the response of the instrument to a known concentration of calibrant gas and establish a calibration factor for the range of expected ambient concentrations of glyoxal.

Figure 2 (Huisman, et al. 2008) illustrates a diagram of the apparatus. The collection or white cell (11) is fastened to an aluminum base (1). Laser light follows a fiber optic to a fiber coupler (4) where it can be aligned properly to the cell. Power from the beam is measured by two photodiodes (2) before it enters the cell itself from laser light that has been sent through a beam splitter and after it travels through the cell along a path dictated by mirrors (3a,b). Laser pulses that enter the white cell are reflected back and forth for a total of 32 passes, which ideally overlap as little as possible. The purpose of sending the same pulse through the same air mixture is based on the desire for a maximum volume of air in front of the PMT to be exposed to laser light, so that the maximum possible volume of air will be phosphorescing. Main flow of ambient air from the inlets is kept at approximately 31 standard liters per minute by an electronic needle valve (5). This translates into a constant

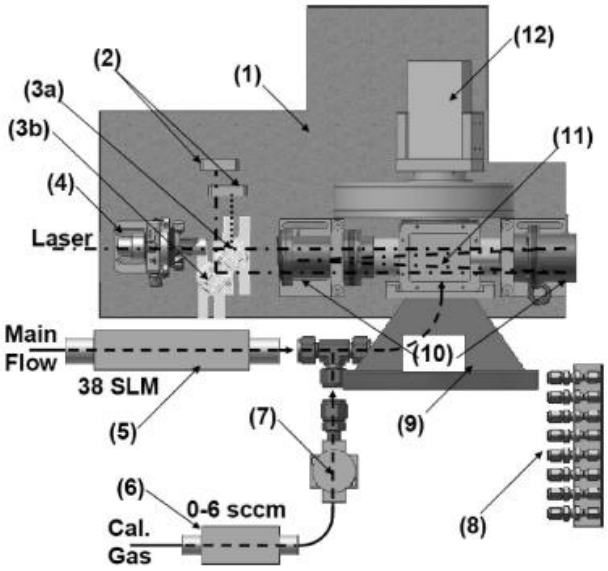

Figure 2. LIP instrument

pressure of 100 torr in the white cell. Phosphorescence efficiency depends strongly on pressure in the cell. Accordingly, there is a trade-off between higher pressures (more intense phosphorescence) and more effective oxygen quenching of the triplet state (less intense phosphorescence). Calibrant gas passes through a 10 sccm flow controller (6) to a Teflon-coated valve (7). UZA gas passes through a manifold (8) before it enters to flush out the cell and keep the optics (10) clean. The PMT (12) is located directly above a light trap (9) and off axis with relation to the laser.

Data Processing

Raw signal counts were collected in 1 second bins and processed using Matlab software. First, 1 Hz data normalized to laser power to eliminate count discrepancies which could result from fluctuations in the laser power. Normalized counts for the 40 second online segments were averaged to obtain "1 minute" averages. Offline signals were calculated as the average of the last 10 seconds of the prior offline segment and the first 10 seconds of the actual 1 minute segment being averaged. Subtracting the averaged offline and online counts yields data which is proportional to the ambient concentration of glyoxal and devoid of interference from background noise. Finally, the power-normalized counts are adjusted using a calibration factor as determined from a standard addition LIP calibration. Floating twenty minute averages are used to eliminate data points that are recorded outside a 3 standard deviation gate and smooth the data.

For inlet comparisons, 1 minute averages underwent additional processing into broader 10 minute averages. Three main inlet collections took place for every one alternate inlet collection and the difference was taken between the most temporally similar values from the inlets.

Results

Data were compiled from July 9th until July 21st, 2008 (Julian days [JD] = 191-203). Main inlet data corresponds to ambient air that was drawn through a fixed glass manifold from the peak elevation of the PROPHET tower. Alternate inlet air was collected through a Teflon-coated tube which was wrapped in aluminum foil to eliminate losses due to photolysis during transport and placed within the canopy at approximately 20 meters in

elevation from July 9th-July 16th (JD 191-198) at 3:30pm. On July 16th, the inlet was lowered to an elevation completely beneath the canopy (approximately 12 meters). Collection took place continuously for the twelve day period, with the only interruptions stemming from calibration periods. Glyoxal concentrations from each location were compared using regression and t test statistical analysis. Ten minute averages were also plotted with meteorological data collected every second during the same period to identify relevant trends.

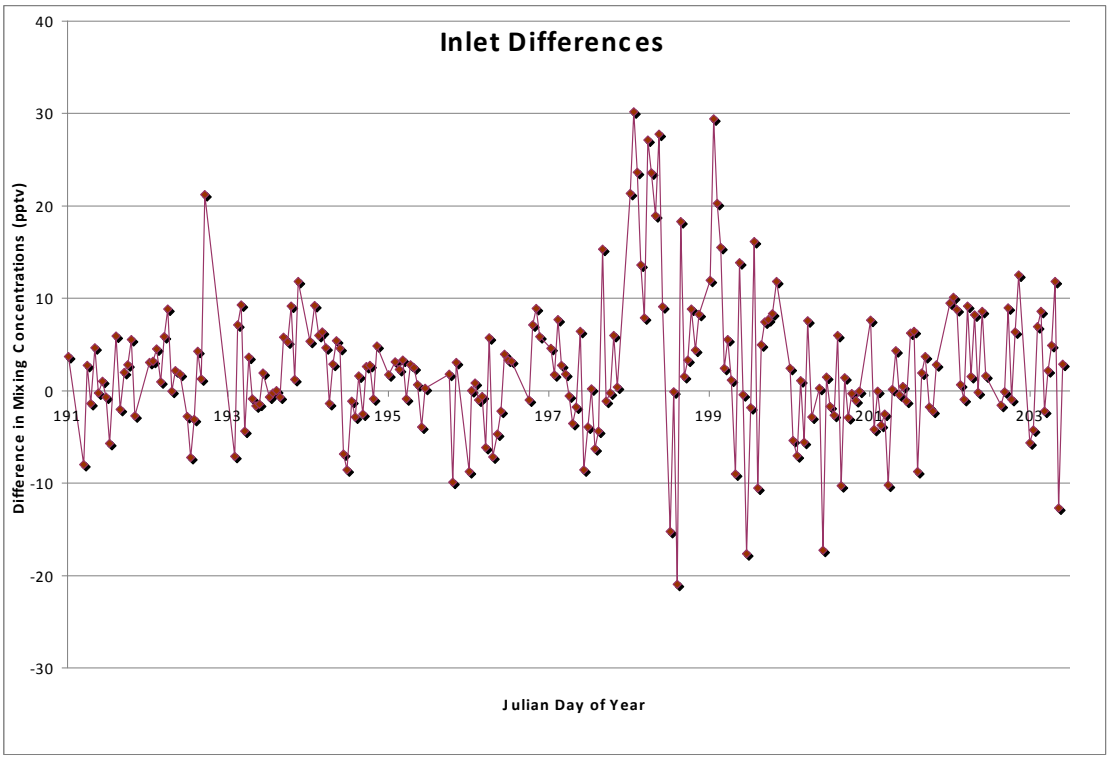

Figure 3. Differences in glyoxal concentrations for the duration of the sampling period.

Differences in glyoxal concentrations between above canopy and within/below canopy collection points are shown in Figure 3. All positive values indicate periods where above canopy concentrations exceeded those below. The greatest average difference (30 parts per trillion mixing concentration) was recorded on July 16th, (JD 198) one day following the shift to a lower collection point. The impact of each sampling location on the total collected concentrations of glyoxal is illustrated in Figure 4. If both sites contained equal concentrations of glyoxal, one would expect to see a consistent division at 50%, with each contributing an equal amount to the whole. Similar to Figure 3, it is evident that a larger contribution is made by the main inlet, which corresponds to the above canopy sampling site.

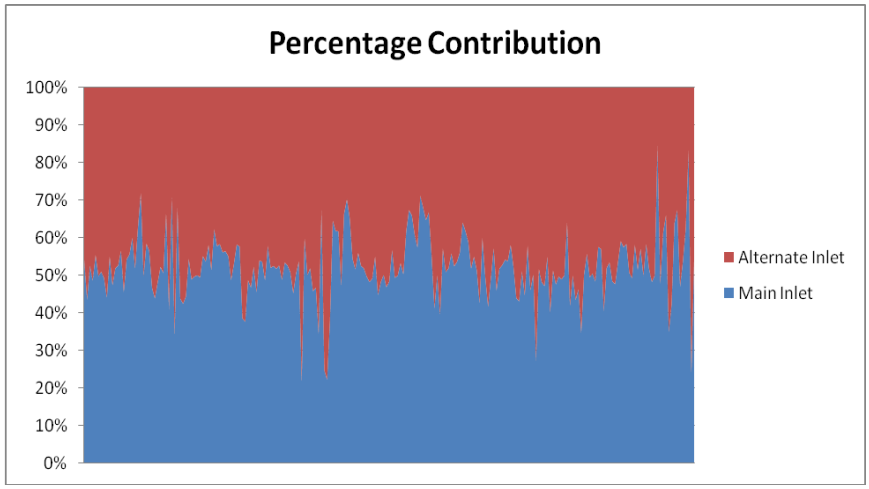

Figure 4. Contribution of each inlet to total measured concentration

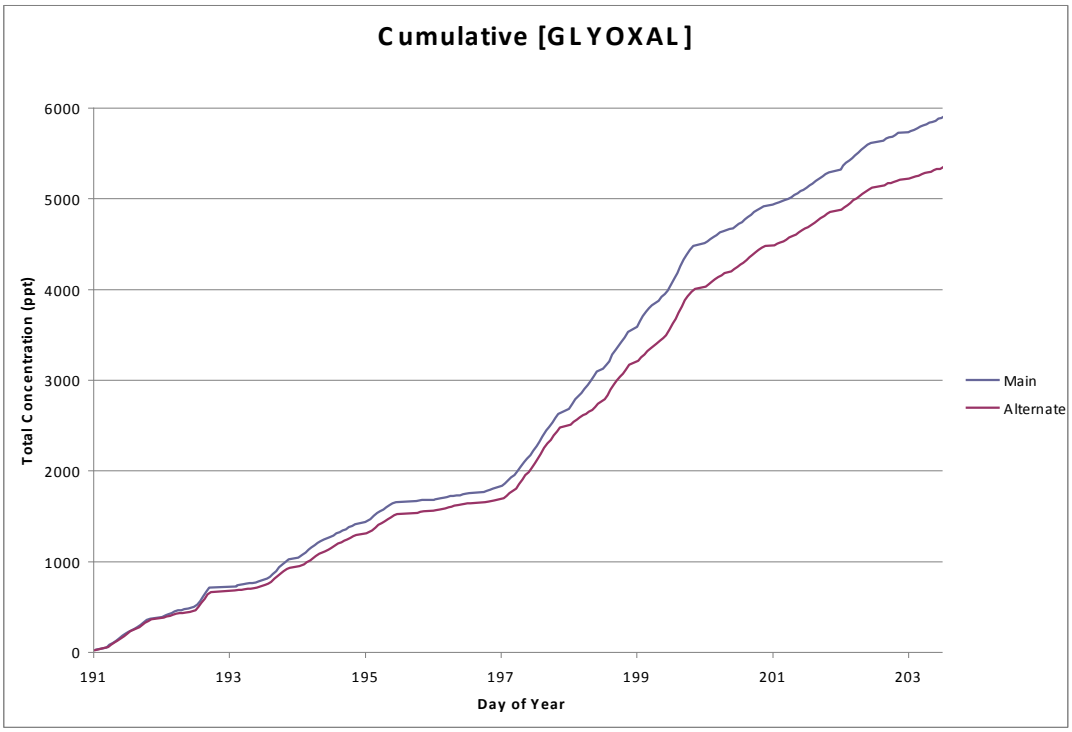

Figure 5. Total concentrations from above (blue) and mid/below (red) the canopy

Collective concentrations of glyoxal from each site are plotted in Figure 5. Throughout the course of sampling, ambient above canopy measurements resulted in a surplus of 561 parts per trillion of glyoxal as compared with the lower testing locations. It is also clear that combined concentrations above the canopy were higher throughout the entire sampling period.

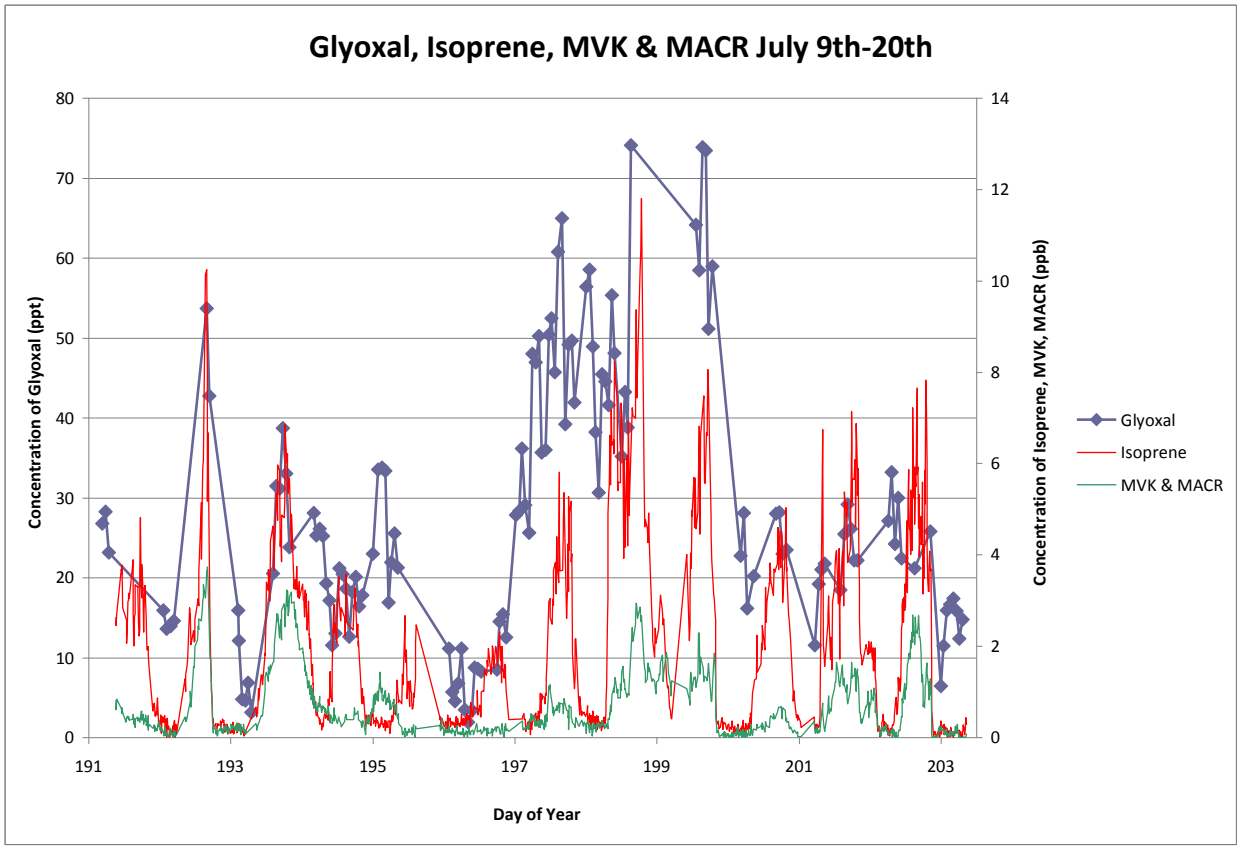

Figure 6. Concentrations of glyoxal (blue), isoprene (red), and MVK & MACR (green)

Continuous measurements of gloxal are plotted in Figure 6 with its primary precursors isoprene, methyl vinyl ketone, and methacrolein (Mielke, 2008). Following the peak daily measurements provides a good indication of the relatedness of each species to one another.

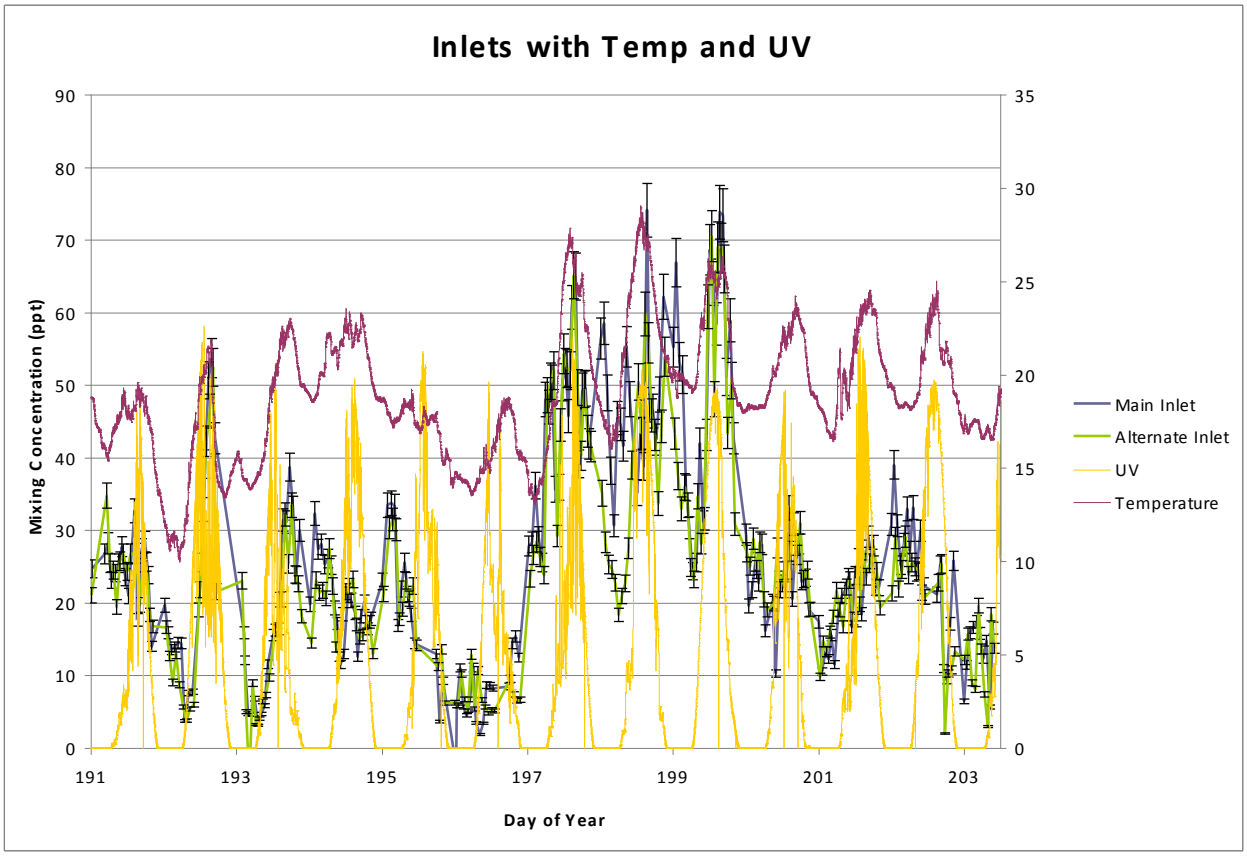

Figure 7. Temperature and UV plotted with [glyoxal]

Concentrations of glyoxal for the full sampling period are plotted alongside temperature and UV data in Figure 7. Taken as a whole, peaks of temperature (degrees C) and UV (W/m^2) tend to track well with glyoxal concentrations from both locations. Some aberrant peaks in [glyoxal] also occur during low temperature/light conditions. For example, early morning on July 13th (JD 195) one can see an unusual peak that corresponds to a dip in temperature and UV data. This will be further addressed in the discussion.

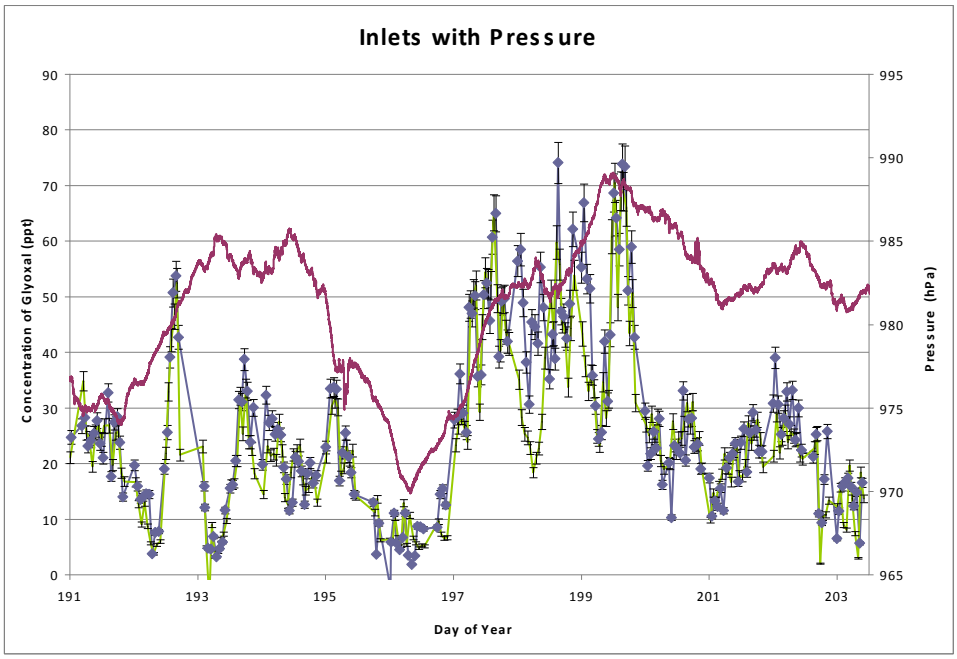

Figure 8. Pressure plotted with [GLYOXAL] for the duration of the sampling period

Atmospheric pressure data is depicted in red in Figure 8. Above canopy (blue) and mid/below canopy concentrations (green) peak are shown with the greatest recorded pressure on July 17th (JD 199).

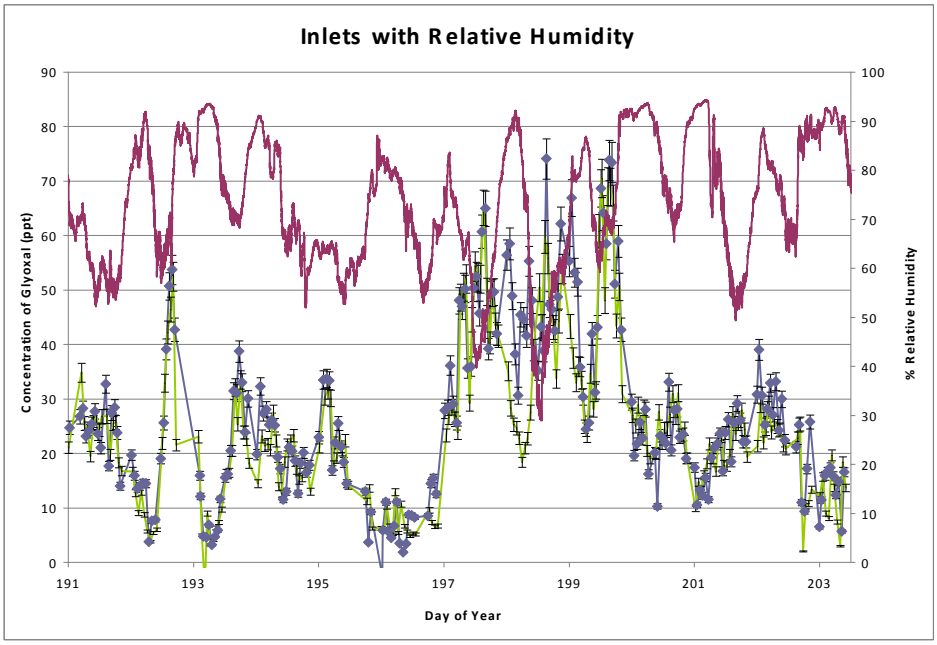

Figure 9. Relative humidity plotted [glyoxal] for the duration of the sampling period

Relative humidity is plotted in Figure 9 with concentrations from above and below that canopy. Rain events are indicated by peaks (over 90%), typically followed shortly thereafter by sharp declines in glyoxal levels.

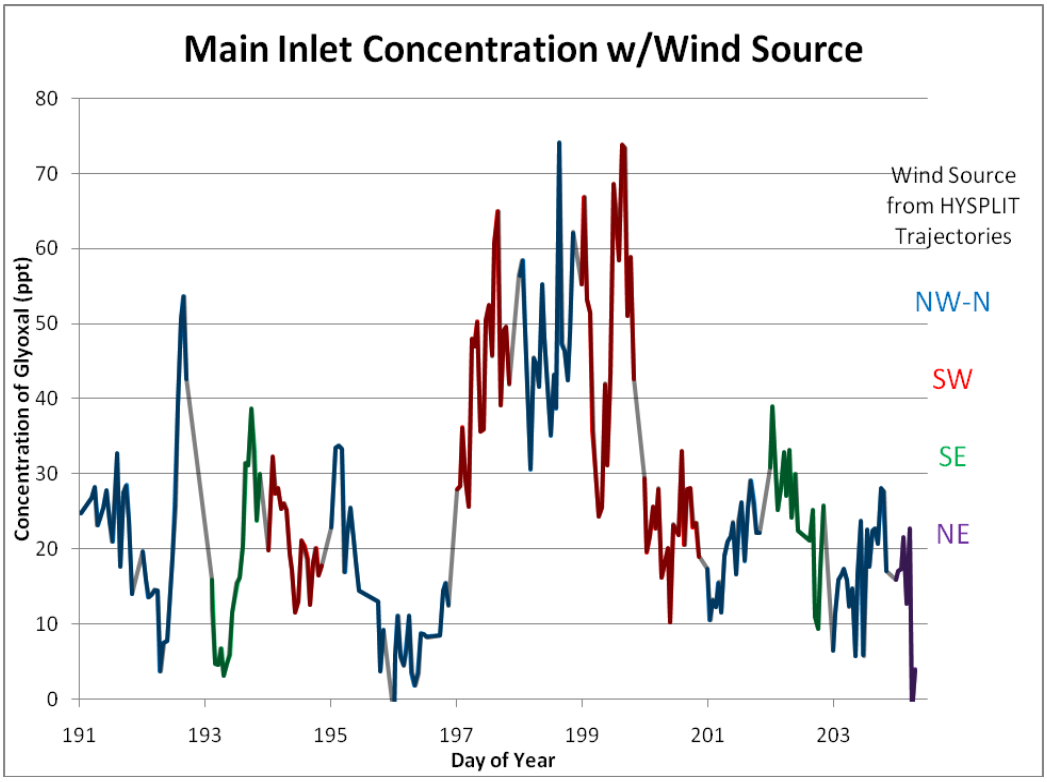

Figure 10. Concentrations of glyoxal according to different air masses

Figure 10 illustrates changing concentrations based on the direction of wind source. PROPHET generally received wind masses from the west, with interruptions from southeast wind masses occurring on two occasions July 11th and July 20th. The highest recorded concentrations were observed from back trajectories corresponding to wind masses that traveled from the southwest, through the Chicago, IL, and Gary, IN, metropolitan/industrial areas.

Analysis

Modeling

Modeling glyoxal concentrations was performed using Matlab software to solve coupled differential equations. Each equation related to a specific source or sink pathway for gloxal and several related species. Parameters including temperature, solar zenith angle, and concentrations of reactants such as OH, O3, etc. provided a somewhat coarse illustration of the behavior of glyoxal in relation to a changing environment.

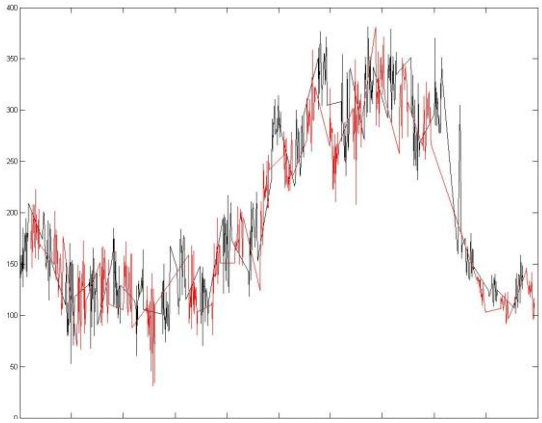

Figure 11. Diurnal cycle of glyoxal

Integrating the change in glyoxal across shorter time periods was performed to attempt to replicate measurements obtained in the field. The characteristic profile of a diurnal glyoxal cycle is portrayed in Figure 11. This used as a starting point for model analyses. This data was collected on a sunny day with warm temperatures. The delayed formation by isoprene oxidation is evident with the late afternoon peak, followed by a sharp drop to relatively constant nighttime concentrations. Black and red data points correspond to different inlets drawing from the same ambient air at equal height. Measurement periods were alternated to ensure that both inlets provided an equal response. Each point corresponds to a one minute average response, which has normalized to laser power, without a calibration factor. Figure 12 displays a basic model which reasonably predicts an expected concentration of glyoxal from the breakdown of isoprene beginning at noon (solar zenith angle = 0), with average temperatures over a 24 hour period.

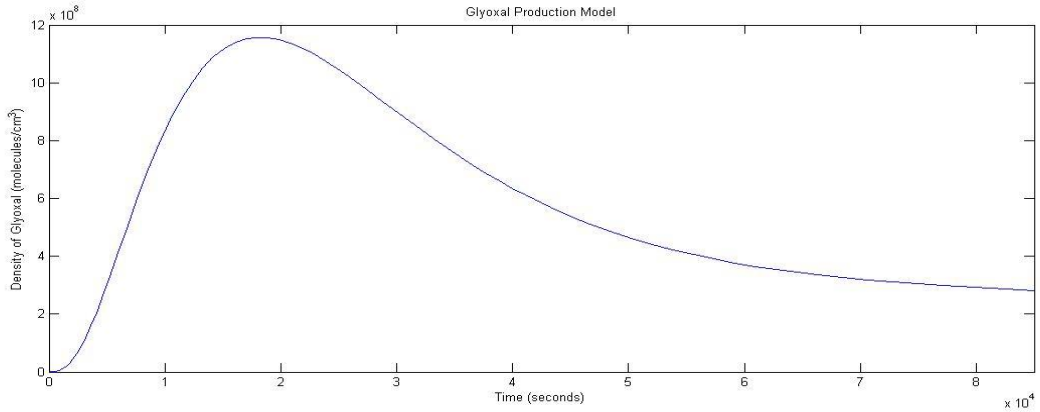

Figure 12. Production and breakdown of glyoxal over 24 hours

The Master Chemical Mechanism v3.1, provided by the University of Leed, was a valuable source for establishing the reaction rates associated with each step of the individual pathways. The model depends on 14 reaction pathways for the creation of glyoxal strictly from a given source of isoprene, which was calculated as a 24 hour average from measured values at the PROPHET site (Mielke 2008). Multiple pathways via key intermediate species such as MVK were utilized with more attention given to OH radical reaction routes. A steady state was assumed for reactions with multiple steps in situations where the intermediate step reaction rate exceeded initial step's reaction rate by 100 fold. Other assumptions include constant atmospheric concentrations of reactants such as OH radical, ozone, CO, RO2, and water vapor. NOx was also included, but in a relatively low concentration, due to the lack of anthropogenic emissions at the PROPHET site. Three sink pathways were included, comprised of three photolysis routes, two OH reaction routes, and two NO3 reaction routes. The final differential equation which explains the concentration of glyoxal is provided below.

```
dy(GLYOXAL) = ((y(HOCH2CHO)*k1_HOCH2CHO) + (y(HOCH2CHO)*k2_HOCH2CHO) + (y(C58NO3)*k3_C58NO3) +
(y(C58O)*k4_C58O) + (y(HC4ACHO)*k5_HC4ACHO) + (y(GLYOO)*k6_GLYOOCO) + (y(GLYOO)*k7_GLYOONO) +
(y(GLYOO)*k8_GLYOO) + (y(GLYOO)*k9_GLYOO) + (y(GLYOO)*k10_GLYOONO2) + (y(HOCH2CHO)*k11_HOCH2CHO)
+ (y(HOCH2CHO)*k12_HOCH2CHO) + (y(GLYOO)*k13_GLYOOCO) + (y(NC4CHO)*k14_NC4CHO)) -
((y(GLYOXAL)*k1_PHOTO) + (y(GLYOXAL)*k2_PHOTO) + (y(GLYOXAL)*k3_PHOTO) + (y(GLYOXAL)*k_GLYOXOH) +
(y(GLYOXAL)*k2_GLYOXOH) + (y(GLYOXAL)*k_GLYOXNO3) + (y(GLYOXAL)*k2_GLYOXNO3));
```

Currently, the model predicts that glyoxal concentrations peak about five hours after isoprene begins to react. Peak concentrations are 46 ppt, reasonable for the PROPHET site. Following the peak, glyoxal decays to a steady level of approximately 15 ppt, somewhat lower than expected. Improvements in the model that would presumably lead to better predicted concentrations include: a dynamic source of isoprene based on field measurements, changing concentrations of relevant reactants, temperature, and UV parameters to simulate diurnal cycles, and a reasonable sink via secondary organic aerosol deposition.

Difference between inlets

Significant differences in glyoxal concentrations were seen in comparisons between above and mid/below canopy inlets. For the initial elevations of this experiment, higher glyoxal concentrations were regularly recorded through the main inlet (eight day average: main inlet = 24.61340551, alt. inlet = 21.96205669, p(two tail) = .0013). Higher mixing

concentrations were also seen through the second portion of the sampling period (five day average: main inlet = 29.54706154, alt inlet = 27.40557692, p(two tail) = .0020). For the entire sampling session, the main inlet averaged higher concentrations of glyoxal, and a robust difference between mean concentrations was confirmed using a two sample paired t test (Table 1) (average: main inlet = 26.74848128, alt. inlet = 24.32176758, p(two tail) = 5.61e-6).

t-Test: Paired Two Sample for Means			t-Test: Paired Two Sample for Means			t-Test: Paired Two Sample for Means		
	Above	*Mid*		*Above*	*Below*		*Above*	*Mid & Below*
Mean	23.79362586	21.89706034	Mean	30.32005248	27.3303802	Mean	26.74848128	24.32176758
Variance	216.7167188	188.8405385	Variance	267.9266969	211.4369853	Variance	252.5018227	206.5257951
Observations	116	116	Observations	101	101	Observations	219	219
Pearson Correlation	0.908052246		Pearson Correlation	0.817837549		Pearson Correlation	0.874779603	
Hypothesized Mean Difference	0		Hypothesized Mean Difference	0		Hypothesized Mean Difference	0	
Df	115		df	100		Df	218	
t Stat	3.306637793		t Stat	3.166164237		t Stat	4.655714136	
P(T<=t) one-tail	0.000630122		P(T<=t) one-tail	0.001023945		P(T<=t) one-tail	2.80391E-06	
t Critical one-tail	1.658211831		t Critical one-tail	1.660234327		t Critical one-tail	1.651873373	
P(T<=t) two-tail	0.001260244		P(T<=t) two-tail	0.00204789		P(T<=t) two-tail	5.60782E-06	
t Critical two-tail	1.980807476		t Critical two-tail	1.983971466		t Critical two-tail	1.970905551	

Table 1. Results of t test analyses

Regression analysis across the within canopy period demonstrated agreeable correlation between inlets, as one would expect (r^2 = .758). A similar correlation between the inlets was observed for the below canopy period (r^2 = .759). Overall correlation was found to be robust between inlet measurements over the entire sampling period (r^2 = .765).

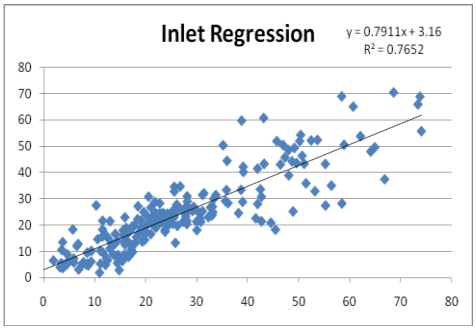

Discussion

Glyoxal mixing concentrations were consistently recorded at higher levels at an above canopy elevation as compared with below canopy ambient air. This pattern can likely be attributed to higher isoprene production near treetops where leaf density reaches its peak, along with more light and heat getting to the leaves. Furthermore, the above canopy environment is conducive to faster oxidation rates resulting from higher direct UV

radiation than the below canopy environment experiences. Absolute differences were commonly lower during rain events and periods of lower average temperatures. This is primarily a result of lower overall ambient concentrations. At the same time, however, the percentage difference between inlets rose slightly with each rain event, indicating that the difference in concentrations never completely disappeared.

Numerous occasions of higher below canopy concentrations were observed in this study (Figure 4). One of the primary drivers behind these observations could have been more diffuse radiation reaching lower levels of the canopy on cloudy days. In this case, one could expect to see higher photosynthetic rates among certain species. Yet, it is difficult to say whether or not this is true, as UV measurements were only available above the canopy.

An additional factor that may have directed observations of higher below canopy glyoxal is the amount of mixing in ambient air. This would have brought above canopy molecules of glyoxal below the canopy, depending on the concentrations associated with each level and, in particular, the speed and pressure associated with the entry of a new air mass. Figure 10 is a rough glimpse at the influence of different sources of air masses, but a deeper investigation may reveal a significant correlation between source and concentrations of glyoxal.

Each of the factors observed in Fig. 7-9 manipulates glyoxal in a unique and relatively significant manner, and should be considered in the creation of an accurate long term model for glyoxal distributions. Tracking observations of inlet concentrations with temperature reveals the particularly strong impact it has on both the initial rate of isoprene production and temperature-dependent reaction rates associated with the formation and breakdown of glyoxal. UV radiation also opens up major pathways for glyoxal formation via photolysis, but also impacts the rate at which it is photolyzed. During the daytime, glyoxal concentrations usually followed a common pattern of peaking in the afternoon. Around the same time, one could observe high incident UV radiation (Fig. 7). Nighttime peaks of glyoxal were highly unanticipated events that demand attention. While there is still not a clear-cut explanation for these phenomena, one could hypothesize that either an anthropogenic source or an uncharacterized primary source may be making these interesting contributions. The importance of relative humidity in forcing ambient concentrations of glyoxal is demonstrated in Figure 3. Generally, higher humidity

dramatically increases the amount of glyoxal that is removed by route of physical deposition, because of the very efficient wet deposition characteristics of glyoxal (Matsumoto et. al, 2005). As measurements were taken in a rural setting, bereft of anthropogenic sources of glyoxal, weather played a central role in forcing the final concentrations that were observed.

Given the established contribution of gloxal to secondary organic aerosols, measurements of aerosol would have been particularly useful in the characterization an addition aspect of glyoxal chemistry. Knowledge of aerosol mass and concentration, overall and within the canopy, would have helped in understanding the role of this important sink for glyoxal. Unfortunately, data had not been analyzed and made available at the time of this writing.

Conclusion

This study demonstrated a clear distinction between the observed concentrations of glyoxal above a deciduous forest canopy when compared with concentrations collected below the canopy. Further directions for research could include the quantitative identification of factors such as ambient air mixing patterns, differences in isoprene production rates, and studies on UV radiation and aerosols within the canopy, all of which may relate to the observed discrepancy between above and below canopy measurements. Other work could could focus on further model development to calculate the concentrations of glyoxal one would anticipate seeing in different types of canopies and at different levels of the canopy itself.

Acknowledgements

This study was supported by the National Science Foundation, which provided funding for the Research Experience for Undergraduates (REU) Program at the University of Michigan Biological Station during the summer of 2008. Much support and guidance was offered from my mentors Aster Kammrath and Melissa Galloway and the Keutsch research group as a whole. I am also appreciative of the instruction from Dave Karowe and Mary Anne Carroll, who, in conjunction with Steve Bertman, also collected meteorological data. Also worth recognition is Fred McNeal for his assistance with back trajectories and the help of Bob Vande Koppel and my fellow REU students.

References

Anderson, L.C., C.S. Parmenter, and H.M. Poland (1973). Collision induced intersystem crossing. The photophysics of glyoxal vapor excited at 4358 Angstroms. Chem. Phys. 1: 401-417.

Bates, T.S., T. L. Anderson, T. Baynard, T. Bond, O. Boucher, G. Carmichael, A. Clarke, C. Erlick, H. Guo, L. Horowitz, S. Howell, S. Kulkarni, H. Maring, A. McComiskey, A. Middlebrook, K. Noone, C. D. O'Dowd, J. Ogren, J. Penner, P. K. Quinn, A. R. Ravishankara, D. L. Savoie, S. E. Schwartz, Y. Shinozuka, Y. Tang, R. J. Weber, and Y. Wu (2006). Aerosol direct radiative effects over the northwest Atlantic, northwest Pacific, and North Indian Oceans: estimates based on in-situ chemical and optical measurements and chemical transport modeling. Atmos. Chem. Phys. 6: 1657-1732.

Boissard, C., F. Chervier, and A. L. Dutot (2008). Assessment of high (diurnal) to low (seasonal) frequency variations of isoprene emission rates using a neural network approach. Atmos. Chem. Phys. 8: 2089-2101.

Cerqueira, M.A., C.A. Pio, P.A. Gomes, J.S. Matos, and T.V. Nunes (2003). Volatile organic compounds in rural atmospheres of central Portugal. Sci. Tot. Environ. 313: 49-60.

Fuentes, J., D. Wang, D. Bowling, M. Potosnak, R. Monson, W. Goliff, and W. Stockwell (2007). Biogenic hydrocarbon chemistry within and above a mixed deciduous forest. J. Atmos. Chem., 56: 165-185.

Ghan, S. and S. Schwartz (2007). Aerosol properties and processes. Amer. Met. Soc. 7: 1059-1083.

Grosjean, D. (1990). Gas-phase reaction of ozone with 2-methyl-2-butene: Dicarbonyl formation from Criegee biradicals**.** Environ. Sci. Technol. 24: 1428-1432.

Grosjean, D., E. L. Williams, and E. Grosjean (1993). Atmospheric chemistry of isoprene and of its carbonyl products. Environ. Sci. Technol. 27: 830-840.

Huisman, A., J. Hottle, K. Coens, J. Digangi, M. Galloway, A. Kammrath, and F. Keutsch (2008). Laser-induced phosphorescence for the in situ detection of glyoxal at part per trillion mixing ratios. Anal. Chem.: 18593190

Karl, T., A. Guenther, R. J. Yokelson, J. Greenberg, M. Potosnak, D. R. Blake, and P. Artaxo (2007), The tropical forest and fire emissions experiment: Emission, chemistry, and transport of biogenic volatile organic compounds in the lower atmosphere over Amazonia, J. Geophys. Res., 112, D18302.

Kim, D., and V. Ramanathan (2008), Solar radiation budget and radiative forcing due to aerosols and clouds, J. Geophys. Res., 113, D02203.

Knohl, A., and D. D. Baldocchi (2008). Effects of diffuse radiation on canopy gas exchange processes in a forest ecosystem. J. Geophys. Res., 113, G02023.

Li, X. and H. Schlegel (2001). Photodissociation of glyoxal: Resolution of a paradox. J. Chem. Phys. 114: 8-10.

Liggio, J., S.-M. Li, and R. McLaren (2005). Reactive uptake of glyoxal by particulate matter. J. Geophys. Res., 110, D10304.

Lohmann, U., and J. Feichter (2005). Global indirect aerosol effects: a review. Atmos. Chem. Phys. 5: 715-737.

Matsumoto, K., S. Kawai, and M. Igawa (2005). Dominant factors controlling concentrations of aldehydes in rain,fog,dew water,and in the gas phase. Atmos. Environ., 39: 7321-7329.

Matsunaga, S. N., A. Guenther, Y. Izawa, C. Wiedinmyer, J. Greenberg, and K. Kawamura (2007). Importance of wet precipitation as a removal and transport process for atmospheric water soluble carbonyls. Atmos. Environ. 41: 790-796.

Mielke, L. (2008) In Preperation

Millet, D. B., D. J. Jacob, K. F. Boersma, T. M. Fu, T. P. Kurosu, K. Chance, C. L. Heald, and A. Guenther (2008), Spatial distribution of isoprene emissions from North America derived from formaldehyde column measurements by the OMI satellite sensor, J. Geophys. Res., 113, D02307.

Muller, J., T. Stavrakou, S. Wallens, I. De Smedt, M. Van Roozendael, M. J. Potosnak, J. Rinne, B. Munger, A. Goldstein, and A. B. Guenther (2008). Global isoprene emissions estimated using MEGAN, ECMWF analyses and a detailed canopy environment model. Atmos. Chem. Phys. 8: 1329-1341.

Ortega, J., D. Helmig, A. Guenther, P. Harley, S. Pressley, and C. Vogel (2007). Flux estimates and OH reaction potential of reactive biogenic volatile organic compounds (BVOCs) from a mixed northern hardwood forest. Atmos. Environ. 41: 5479-5495.

Possanzini, M., G. Tagliacozzo, and A. Cecinato (2007). Ambient levels and sources of lower carbonyls at Montelibretti, Rome (Italy). Water Air Soil Pollut. 183: 447-454.

Ho, K.F., S.C. Lee, J.J. Cao, K. Kawamura, T. Watanabe, Y. Cheng, and J. Chow (2006) Dicarboxylic acids, ketocarboxylic acids, and dicabonyls in the urban roadside area of Hong Kong. Atmos. Environ. 40: 3030-3040.

Pressley, S., B. Lamb, H. Westberg, J. Flaherty, J. Chen, and C. Vogel (2005). Long-term isoprene flux measurements above a northern hardwood forest. J. Geophys. Res., 110, D07301.

Serebrennikov, L.V., A.V. Golovkin, M.V. Polyakova, and V.F. Shevel'kov (2001) Infrared chemiluminescence spectra of gas-phase products from the reaction between glyoxal and hydrogen peroxide. Russ. J. Phys. Chem. 75: 543-550.

Sinreich, R., R. Volkamer, F. Filsinger, U. Frieß, C. Kern, U. Platt, O. Sebastian, and T. Wagner (2007). MAX-DOAS detection of glyoxal during ICARTT 2004. Atmos. Chem. Phys., 7: 1293–1303.

Sumner, A., P. Shepson, T. Couch, T. Thornberry, M.A. Carroll, S. Sillman, M. Pippin, S. Bertman, D. Tan, I. Faloona, W. Brune, V. Young, O. Cooper, J. Moody, and W. Stockwell (2001). A study of formaldehyde chemistry above a forest canopy. J. Geophys. Res., 106: 24387-24405.

Tadic, J., G. Moortgat, and K. Wirtz (2006). Photolysis of glyoxal in air. Journal of Photochemistry and Photobiology A: Chemistry 177: 116-124.

Volkamer, R., L. Molina, M. Molina, T. Shirley, and W. Brune (2005). DOAS measurement of glyoxal as an indicator for fast VOC chemistry in urban air. Geophys. Res. Lett., 32, L08806.

Volkamer, R., U. Platt, and K. Wirtz (2001). Primary and Secondary Glyoxal Formation from Aromatics: Experimental Evidence for the Bicycloalkyl-Radical Pathway from Benzene, Toluene, and p-Xylene. J. Phys. Chem. A 2001, 105, 7865-7874.

Volkamer, R., F. San Martini, L. T. Molina, D. Salcedo, J. L. Jimenez, and M. J. Molina (2007). A missing sink for gas-phase glyoxal in Mexico City: Formation of secondary organic aerosol. Geophys. Res. Lett., 34, L19807.

Wittrock, F., A. Richter, H. Oetjen, J. P. Burrows, M. Kanakidou, S. Myriokefalitakis, R. Volkamer, S. Beirle, U. Platt, and T. Wagner (2006), Simultaneous global observations of glyoxal and formaldehyde from space, Geophys. Res. Lett., 33, L16804.